Journal of Translational Medicine

RESEARCH

Open Access

Innovative biomarkers TCN2 and LY6E can significantly inhibit respiratory syncytial virus infection

Bochun Cao[1,3†], Menglu Li[6†], Xiaoping Li[4†], Xianyan Ji[1], Lin Wan[1], Yingying Jiang[1], Lu Zhou[5], Fang Gong[1*] and Xiangjie Chen[1,2,3*]

Abstract

Background Respiratory syncytial virus (RSV) is a prominent etiological agent of lower respiratory tract infections in children, responsible for approximately 80% of cases of pediatric bronchiolitis and 50% of cases of infant pneumonia. Despite notable progress in the diagnosis and management of pediatric RSV infection, the current biomarkers for early-stage detection remain insufficient to meet clinical needs. Therefore, the development of more effective biomarkers for early-stage pediatric respiratory syncytial virus infection (EPR) is imperative.

Methods The datasets used in this study were derived from the Gene Expression Omnibus (GEO) database. We used GSE188427 dataset as the training set to screen for biomarkers. Biomarkers of EPR were screened by Weighted Gene Co-expression Network Analysis (WGCNA), three machine-learning algorithms (LASSO regression, Random Forest, XGBoost), and other comprehensive bioinformatics analysis techniques. To evaluate the diagnostic value of these biomarkers, multiple external and internal datasets were employed as validation sets. Next, an examination was performed to investigate the relationship between the screened biomarkers and the infiltration of immune cells. Furthermore, an investigation was carried out to identify potential small molecule compounds that interact with selected diagnostic markers. Finally, we confirmed that the expression levels of the selected biomarkers exhibited a significant increase following RSV infection, and they were further identified as having antiviral properties.

Results The study found that lymphocyte antigen 6E (LY6E) and Transcobalamin-2 (TCN2) are two biomarkers with diagnostic significance in EPR. Analysis of immune cell infiltration showed that they were associated with activation of multiple immune cells. Furthermore, our analysis demonstrated that small molecules, 3′-azido-3′-deoxythymine, methotrexate, and theophylline, have the potential to bind to TCN2 and exhibit antiviral properties. These compounds may serve as promising therapeutic agents for the management of pediatric RSV infections. Additionally, our data revealed an upregulation of LY6E and TCN2 expression in PBMCs from patients with RSV infection. ROC analysis indicated that LY6E and TCN2 possessed diagnostic value for RSV infection. Finally, we confirmed that LY6E and TCN2 expression increased after RSV infection and further inhibited RSV infection in A549 and BEAS-2B

†Bochun Cao, Menglu Li and Xiaoping Li these authors contributed equally.

*Correspondence:
Fang Gong
gongfang2004@163.com
Xiangjie Chen
9862023157@jiangnan.edu.cn
Full list of author information is available at the end of the article

cell lines. Importantly, based on TCN2, our findings revealed the antiviral properties of a potentially efficacious compound, vitamin B12.

Conclusion LY6E and TCN2 are potential peripheral blood diagnostic biomarkers for pediatric RSV infection. LY6E and TCN2 inhibit RSV infection, indicating that LY6E and TCN2 are potential therapeutic target for RSV infection.

Keywords LY6E, TCN2, Respiratory syncytial virus (RSV), Pediatric RSV infection, Biomarker

Introduction

Respiratory tract infection is a common pediatric ailment and a leading cause of pediatric hospital admissions [1, 2]. The underdeveloped humoral immune system in children hinders the production of secretory IgA in the respiratory mucosa, rendering them vulnerable to respiratory tract infections and pulmonary inflammation. Respiratory Syncytial Virus (RSV), a single negative-stranded RNA virus classified under the pneumovirus genus, is a prominent pathogen responsible for pediatric respiratory infections [3, 4]. Many researchers suggest that RSV infection is responsible for ~ 80% of cases of pediatric bronchiolitis and 50% of cases of infant pneumonia [5, 6]. The majority of children infected with RSV exhibit mild upper respiratory tract symptoms or are asymptomatic [7]. However, a significant portion of pediatric RSV patients, approximately one-third, develop acute lower respiratory tract infections such as bronchiolitis or pneumonia [8]. In individuals with chronic lung disease, congenital heart defects, or other comorbidities, RSV infection can present a serious and potentially life-threatening risk [9]. In order to enhance the management of pediatric RSV infections, it is imperative to enhance early detection capabilities for RSV infection. Presently, clinical diagnosis of RSV infection primarily relies on PCR for viral RNA detection [10], yet this method is hindered by numerous limitations such as complexity, time consumption, and vulnerability to cross-contamination. Consequently, rapid RSV antigen detection is commonly employed in clinical diagnosis for pediatric RSV infection, however, its principal drawback lies in its reduced accuracy, particularly in terms of poor sensitivity for detecting early-stage RSV infections [11]. Hence, it is imperative to develop more effective biomarkers for early-stage pediatric RSV infection (EPR).

RSV infection can lead to differential gene expression in the host cells, which may be potential biomarkers of RSV infection. The identification and evaluation of differentially expressed genes (DEGs) with diagnostic significance may offer novel biomarkers for early-stage prediction of RSV infection. Integrating these biomarkers into existing clinical detection methods could improve the precision of RSV infection diagnosis. Recent studies have explored the development of innovative diagnostic biomarkers for RSV infection. For example, certain neurotrophins, cytokines, and cell metabolites have been identified as potential biomarkers for RSV infection [12–14]. The levels of piR-32678 and piR-59169 small non-coding RNAs following RSV infection may serve as indicators of the host response to the virus [15]. Additionally, alterations in the expression levels of various microRNAs in the serum of RSV-infected individuals suggest their potential utility as biomarkers and prognostic indicators for RSV infection [15, 16]. Further investigation into the biological roles of these differentially expressed host components during RSV infection is warranted. For instance, the E3 ubiquitin ligase DTX3L is induced following RSV infection, leading to the enhancement of IFN-I production, which hinders RSV replication [17]; on the other hand, Siglec-1 is significantly upregulated post-RSV infection and hampers T cell activity, aiding in RSV immune evasion [18]. Collectively, the comprehensive analysis of DEGs during RSV infection is essential not only for the discovery of potential diagnostic indicators for RSV infection but also for elucidating the roles these molecules play in the pathogenesis of RSV, thus unveiling potential therapeutic targets.

Transcriptomics sequencing has emerged as a dependable method for investigating disease biomarkers and pathogenesis. Numerous publicly accessible databases aid in elucidating the biological roles of DEGs in various diseases. Utilizing machine-learning algorithms to analyze these DEGs enables the efficient evaluation of complex datasets and the identification of genes with significant biological relevance [19]. Currently, machine-learning algorithms are extensively utilized in the exploration of novel biomarkers for diseases like inflammatory bowel disease, rheumatoid arthritis and Alzheimer's disease, and demonstrating notable advantages in research endeavors [20–22].

Here, we analyzed the DEGs in EPR using publicly available databases and conducted bioinformatics analysis to identify Lymphocyte antigen 6E (LY6E) and Transcobalamin-2 (TCN2) as potential key genes involved in RSV infection. Subsequently, we conducted

experimental studies to investigate the upregulation of TCN2 and LY6E expression in response to RSV infection and confirmed their biological roles in inhibiting viral infection. Overall, our findings highlighted TCN2 and LY6E as potential biomarkers for EPR and demonstrated their antiviral functions, suggesting their potential as targets for clinical diagnosis and treatment of EPR.

Methods

Human samples

This study comprised a cohort of 21 healthy individuals and 23 patients diagnosed with RSV infection. The research was conducted in strict adherence to a protocol approved by the Ethics Committee of Jiangnan University Medical Center, with informed consent obtained from all participants. Patient recruitment was facilitated through the outpatient clinic of Jiangnan University Medical Center, with an admission time of less than 24 h. Blood samples were collected, and peripheral blood mononuclear cells (PBMCs) were subsequently isolated using the Lymphocyte Separation Medium (DAKEWE, Shenzhen, China, 7111011), following the manufacturer's guidelines.

Data acquisition

Standardized gene expression matrices were downloaded from the GEO database to study the DEGs in RSV infection whole blood transcriptomic dataset (GSE188427, GSE80179, GSE105450 and GSE77087). GSE188427 dataset contained 198 samples included healthy control (HC) group (51 samples) and EPR group (147 samples). GSE80179 dataset contained 79 samples included HC group (52 samples) and RSV infection group (27 samples). GSE105450 dataset contained 127 samples included HC group (38 samples) and RSV infection group (89 samples). GSE77087 dataset contained 104 samples included HC group (23 samples) and RSV infection group (81 samples).

Analysis of differential genes

Use the R package "limma" to screen DEGs between RSV infection and HC groups and generated volcanic points or heat maps to visualize DEGs. DEGs was screened according to "adjusted $P < 0.05$" and "$|\log2FC| > 0.5$", and created heat maps by "complexpheatmap" package.

Functional correlation analysis

Gene Ontology (GO) enrichment analysis was used to understand the biological processes (BP), cell components (CC) and molecular functions (MF) of DEGs. Kyoto Encyclopedia of Genes and Genomes (KEGG) enrichment analysis was used to study the signaling pathways involved in DEGs. GO and KEGG enrichment analyses were performed using the "clusterProfiler" and "org.Hs.eg.db" packages, the screening criterion was $P(adj) < 0.05$. Visualizing enrichment analysis results used "ggplot2" and "GOplot" packages.

Weighted gene co-expression network analysis (WGCNA)

WGCNA was carried out to build modules related to EPR based on the gene expression profiles. After calculating the Pearson correlation coefficient, the similarity matrix was constructed. Then, choose the soft threshold = 10, converted the similarity matrix to the adjacency matrix, and next convert the adjacency matrix to the topological overlap matrix (TOM). TOM was used for average-linkage hierarchical clustering to classify gene modules, with each module containing at least 100 genes. After merging similar gene modules, a total of 12 distinct modules were obtained, with the magenta module being considered the core module. The "VennDiagram" package was used to visualize genes shared by WGCNA and DEGs.

Machine-learning algorithm screening for biomarkers

Three machine-learning algorithms, Least Absolute Shrinkage and Selection Operator (LASSO), Random Forests (RF) and eXtreme Gradient Boosting (XGBoost), were used to screen EPR biomarkers. The "glmnet" package was used for LASSO regression analysis, tenfold cross-validation was adopted, and the minimum lambda value was used as the optimal solution. RF analysis was performed using the "randomForest" package. XGBoost analysis using the "XGBoost" package.

Evaluation and correlation analysis of infiltration-related immune cells

CIBERSORT algorithm was used to compare the characteristics of immune cell infiltration in EPR and HC groups. CIBERSORT algorithm analyzed tissue expression matrix by linear support vector regression and accurately quantified the number of 22 types of immune cells in each sample. Using the "CIBERSORT" package, set "perm = 1000" and the "QN argument" to "TRUE". The "ggh4x" and "ggplot2" packages were used to help visualize the relationship between biomarker expression and immune cell infiltration.

Molecular docking using AutoDock Vina

Drugs corresponding to those diagnostic biomarkers were retrieved using the Enrichr (https://maayanlab.cloud/Enrichr/) database to confirm potential RSV treatment drugs. Crystal structures of those diagnostic biomarkers were obtained from Protein Data Bank (PDB) database (https://www.rcsb.org/). Download the 3D structure of small molecule drugs from PubChem (https://pubchem.ncbi.nlm.nih.gov/) or ChemSpider

(http://www.chemspider.com/) database. Autodock Vina software was used for molecular docking, and the results were visualized using Pymol software.

Cell culture, maintenance, and transfection

The A549 and BEAS-2B cell lines were purchased from National Collection of Authenticated Cell Cultures (Shanghai, China), the Hep2 cells was a gift from Dr. Li. Cells were cultured at 37 ℃ under 5% CO_2 in Dulbecco's modified Eagle medium (Gibco, Grand Island, America) or 1640 RPMI Medium (Gibco) with 10% FBS (Vazyme, Nanjing, China, F101-01), 100 μg/mL streptomycin and 100 U/mL penicillin (Biosharp, Hefei, China, BL505A). All transient transfections were performed using the Lipofectamine™ 2000 (Invitrogen, California, America, 11668) on the basis of the manufacturer's instructions.

Expression constructs and reagents

Human TCN2 and LY6E genes were amplified by PCR in the laboratory and constructed on pcDNA3.1 plasmid vector. The shRNAs targeting LY6E and TCN2 were constructed in the laboratory and constructed on pLVX-shRNA2 plasmid vector. The shLY6E targeting sequence was TTCTGGATCCCACAGTGTATG, the shTCN2 targeting sequence was CTGAACCACAAGACCTACATT. Vitamin B12 purchased from Sangon Biotech (Shanghai, China, A502484-0001). 3′-Azido-3′-deoxythymidine (B33784), Dexamethasone (B25793), Theophylline (B20144) and Methotrexate (B25455) purchased from Yuanye Bio-Technology Company (Shanghai, China). All compounds were dissolved in DMSO, and stored at − 80 ℃.

Western Blot analysis

RIPA lysate (Beyotime, Shanghai, China, P0013D) and PMSF (50 μg/mL) were mixed as lysate buffer to harvest A549 cells. As previously mentioned, western blot was used to evaluate protein expression [23]. The following antibodies are used: Flag (1:5000, F7425, Sigma, St. Louis, America), Respiratory Syncytial Virus M2-1 protein (1:1000, ab94805, Cambridge, America), Tubulin (1:10,000, T0023, Affinity, Changzhou, China).

RSV (L19 strain) preparation and infection

RSV preparation and infection were referred to the methods of Jiaqi Huang et al. [17].

RNA isolation and RT-qRCR

Total RNAs were extracted using TRIzol reagent (Vazyme, R401-01) according to the product instructions. All cDNA was synthesized from 600 ng of total RNA using HiScript III Reverse Transcriptase (Vazyme, R312). Then, the mRNA levels were analyzed by RT-qPCR using indicated primers and ChamQ SYBR Color qPCR Master Mix (Vazyme, Q411-02). Primers were designed using Primer 3.0 online website, and all primers showed great species specificity. RT-qPCR analysis was performed by a two-step RT-qPCR method, and the relative expression of target genes was normalized to GAPDH mRNA [24].

The primer sequences were as follows:

TCN2, 5′-cagaacagtgcgagaggagatc-3′ and 5′-tcgccttgagacatgctgttcc-3′;

LY6E, 5′-gaccaggacaactactgcgtga-3′ and 5′-aagccacaccaacattgacgcc-3′;

GAPDH, 5′-gtctcctctgacttcaacagcg-3′ and 5′-accaccctgttgctgtagccaa-3′;

RSV F (RSV fusion protein), 5′-gaattgcagttgctcatgcaa-3′ and 5′-tggcgattgcagatccaaca-3′;

RSV M2-1 (RSV Matrix protein 2-1), 5′-aagtggagctgcagagttgg-3′ and 5′-gtgaggagtttgctcatggc-3′.

Immunofluorescence

Cells were infected with RSV-mCherry (a strain of RSV L19 containing a mCherry gene) for 20 h. Then, cells were subjected to analysis by immunofluorescence microscopy. The fluorescent images were captured with the Olympus IXplore. The images were magnified at 100×.

Statistical analysis

Data analysis was performed using GraphPad Prism 9.0 software. Different groups were compared by a two-tailed Student's T-test or one-way analysis of variance. All differences were regarded as statistically significant when $^{*}p < 0.05$, $^{**}p < 0.01$, $^{***}p < 0.001$.

Results

Screening of DEGs in EPR

The research process of this study was shown in Figure S1. To identified DEGs associated with EPR, an mRNA expression microarray (GSE188427) was obtained from the GEO database. The raw microarray data was normalized to ensure uniform expression levels across all samples (Figure S2). Subsequently, the "limma" package was utilized for the analysis of DEGs between the EPR and HC groups. A total of 477 DEGs were identified, consisting of 398 upregulated genes and 79 downregulated genes in the EPR group compared to the HC group. The volcano plot (Fig. 1A) was employed to visually represent genes exhibiting significant differences in expression levels between the EPR and HC groups. In order to enhance comprehension of the biological roles fulfilled by the DEGs, KEGG and GO enrichment analyses were performed. The KEGG enrichment analysis revealed that the DEGs were primarily linked to the NOD-like receptor signaling pathway, Lipid and atherosclerosis, Toll-like

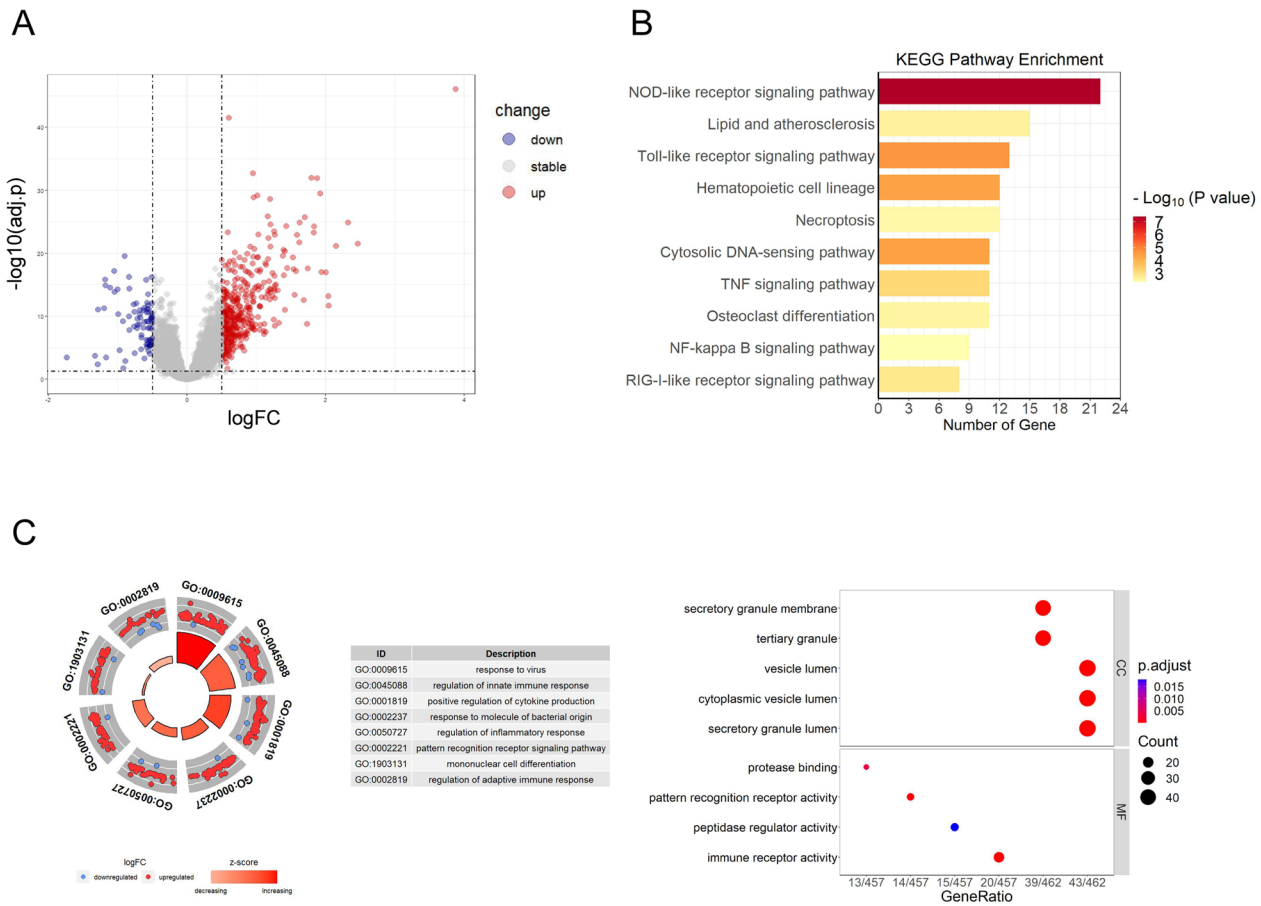

Fig. 1 DEGs of EPR were identified and functional enrichment analysis was performed. **A** The volcano plot showed 477 DEGs between the EPR and HC groups in the GSE188427 dataset. **B, C** Functional enrichment revealed a significant association between DEGs and host immunity. The enrichment analysis of DEGs was performed by KEGG (**B**) and GO (**C**)

receptor signaling pathway, Hematopoietic cell lineage, Necroptosis, Cytosolic DNA-sensing pathway, TNF signaling pathway, Osteoclast differentiation, NF-kappa B signaling pathway and the RIG-I-like receptor signaling pathway (Fig. 1B). Results from the GO analysis demonstrated that these DEGs were correlated with various biological processes including adaptive immune response, mononuclear cell differentiation, pattern recognition receptor signaling pathway, inflammatory response, bacterial infection, cytokine production, innate immune response, and viral infection. In terms of cell components, DEGs were principally associated with the secretory granule membrane, tertiary granule, vesicle lumen, cytoplasmic vesicle lumen and secretory granule lumen. As for molecular function, protease binding, pattern recognition receptor activity, peptidase regulator activity and immune receptor activity were the most enriched terms (Fig. 1C).

Identification of co-expression gene modules in EPR

WGCNA analysis is to first establish a gene co-expression network, followed by the identification of gene modules that are significantly correlated with EPR within this network. Subsequently, genes that are highly associated with EPR are identified [25]. To assign co-expression genes, the "average correlation degree" and "Pearson correlation values" were calculated to cluster the samples in the dataset with outliers removed (Fig. 2A). Then, based on scale independence of > 0.85, we chose 10 as the "soft threshold power β" to ensure the creation of biologically significant scale-free networks (Fig. 2B). Twelve modules were identified by hierarchical clustering analysis and dynamic TreeCut (Fig. 2C, D). The result of the module-trait correlation analysis indicated a significant positive correlation between the magenta module and EPR, leading to its selection for further investigation (Fig. 2E).

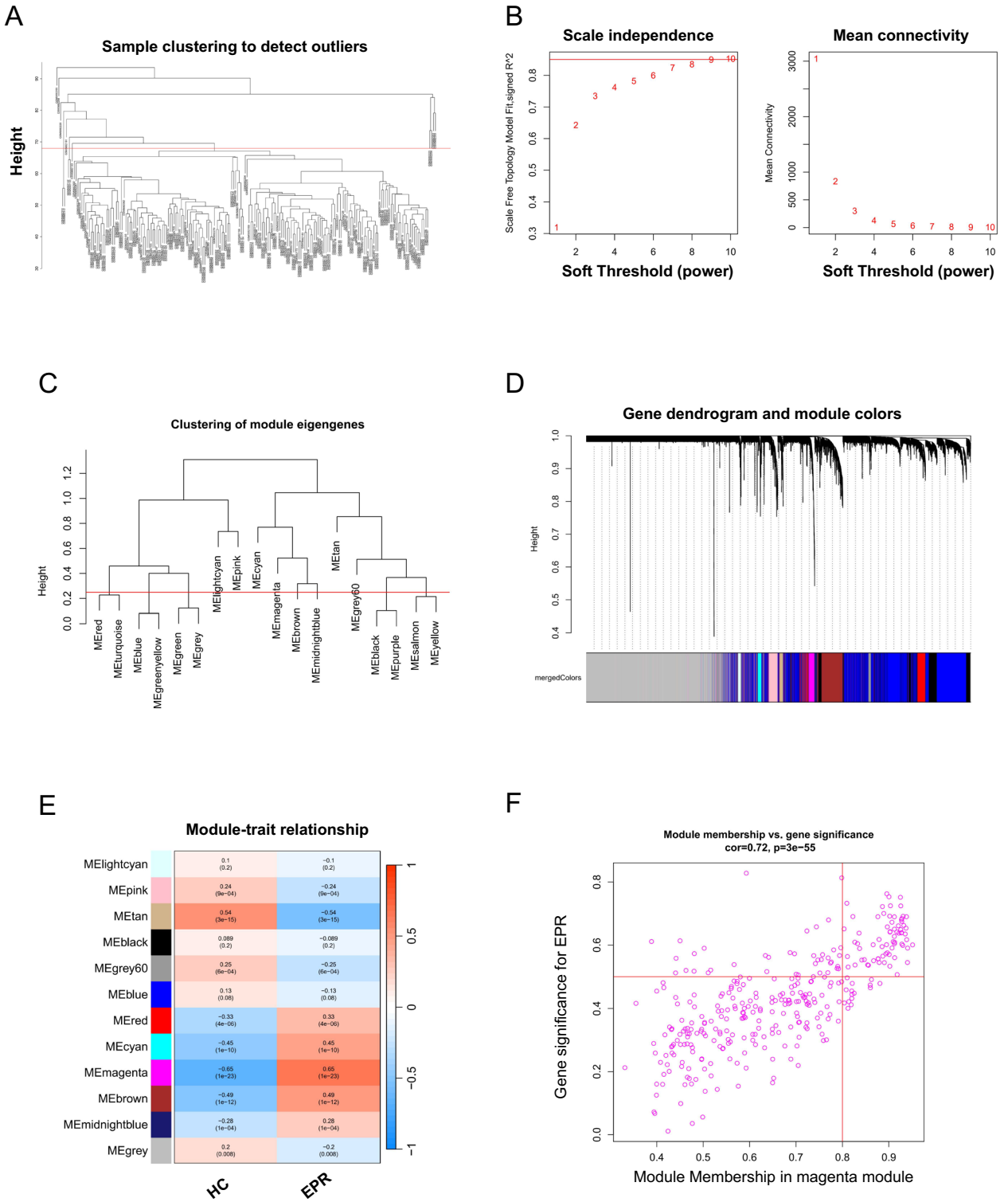

Fig. 2 Construction of weighted co-expression network-related datasets in EPR. **A** A cluster tree of 198 samples. **B** Analysis of network topology for various soft thresholds (β). **C** Clustering dendrogram of genes. **D** Gene dendrograms from average linkage hierarchical clustering. **E** Module-trait relationships. **F** A scatterplot of gene significance for recurrence vs. module membership in the magenta module

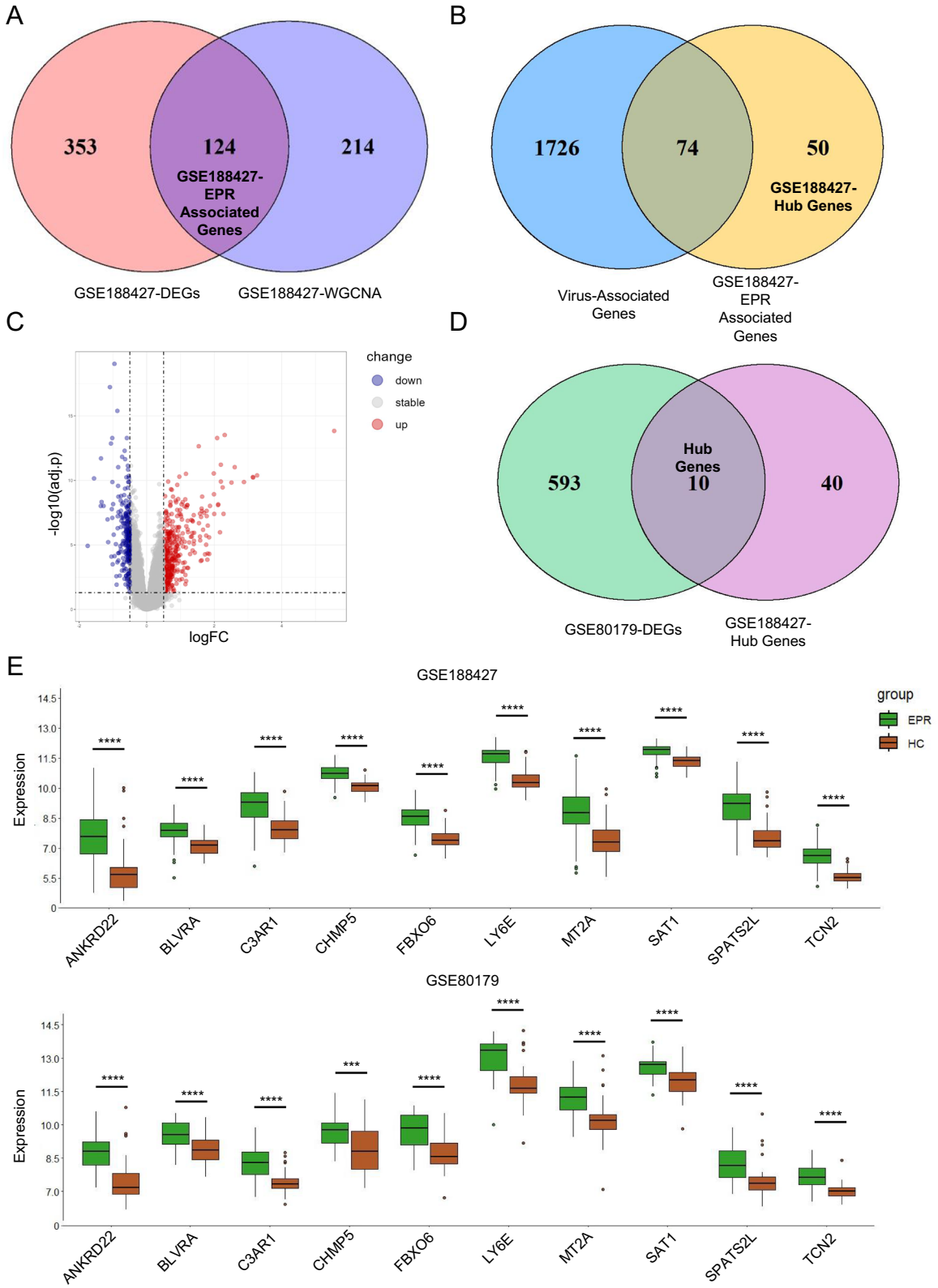

Fig. 3 Selecting ten key genes as EPR hub genes. **A** Venn diagram of magenta module genes versus GSE188427-DEGs. **B** Venn diagram of Virus-Associated Genes versus GSE188427-EPR Associated Genes. **C** The volcano plot showed 603 DEGs between pediatrics RSV infection and HC groups in the GSE80179 dataset. **D** Venn diagram of GSE80179-DEGs versus GSE188427-Hub Genes. **E** The expression levels of ten Hub genes were verified, and the boxplot showed that the expression of these ten genes increased after pediatric RSV infection

Within the magenta module, a total of 338 genes were identified, with a scatter plot demonstrating a strong correlation between these genes and EPR (Fig. 2F). A Venn diagram was utilized to examine the overlap between DEGs and the magenta module genes in the GSE188427 dataset, revealing 124 shared genes (Fig. 3A). These 124 genes were designated as "GSE188427-EPR Associated Genes", and their expression patterns were visualized through heat maps (Figure S3).

Ten key genes were screened as EPR Hub genes

To further identify novel biomarkers for differential expression of RSV after infection, we searched genes in MsigDb with "Virus" as key word. A total of 1800 virus-associated genes were identified. These retrieved genes are highly correlated with the infection of various viruses and play biological functions in the process of viral infection. Our study revealed that a subset of the 124 genes examined exhibited significant associations with viral infections, including IFIT1, IFIT2, STAT1 and RSAD2 et.al, and demonstrated upregulation across a wide range of viral infections. Utilizing Venn diagram for comparative analysis between virus-associated genes and GSE188427-EPR Associated Genes, we identified 50 genes exhibiting a strong correlation with EPR. These genes, previously underreported in relation to viral infections, showed promise as potential biomarkers for EPR and were henceforth referred to as GSE188427-Hub Genes (Fig. 3B). Subsequently, an additional dataset (GSE80179) was obtained from the GEO database, and the "limma" package was employed to analyze the DEGs between the RSV infection and HC groups. A total of 603 DEGs were discerned between the RSV infected and HC groups, with the visualization of these genes facilitated through a volcano plot (Fig. 3C). By employing a Venn diagram to analyze the intersecting areas of GSE80179-DEGs and GSE188427-Hub Genes, we identified 10 common genes (Fig. 3D). Subsequently, an independent sample T-test was conducted to assess the expression discrepancies of these 10 hub genes between the EPR and HC groups. Results from the datasets GSE188427 and GSE80179 revealed that all 10 hub genes exhibited significant upregulation in the EPR group as opposed to the HC group (Fig. 3E).

Screening and validation of diagnostic markers

Three distinct machine-learning algorithms, including LASSO, RF, and XGBoost, were employed to discover potential diagnostic biomarkers for EPR. The LASSO regression algorithm was utilized to construct a model, resulting in the selection of three genes (Fig. 4A, B). Similarly, the RF algorithm was employed to construct a model, leading to the selection of two genes (Fig. 4C, D). Additionally, the XGBoost algorithm was utilized to construct a model, resulting in the selection of two genes (Fig. 4E–G). Ultimately, the three algorithms collectively identified TCN2 and LY6E as RSV infection-related genes. To determine the potential diagnostic value of TCN2 and LY6E genes for pediatric RSV infection, we performed receiver operating characteristic curve (ROC) analysis. In dataset GSE188427, the area under the curve (AUC) of LY6E and TCN2 were > 0.9 (Fig. 5A); in dataset GSE80179, the AUC of LY6E and TCN2 were > 0.8 (Fig. 5B). In dataset GSE105450, the AUC of LY6E and TCN2 were ≥ 0.9 (Fig. 5C); In dataset GSE77087, the AUC of LY6E and TCN2 were > 0.9 (Fig. 5D). Overall, LY6E and TCN2 had consistently demonstrated great diagnostic value across four datasets, suggesting they could be considered as potential "biomarkers" for the diagnosis of pediatric RSV infection.

Analysis of immune cell infiltration

Furthermore, we utilized the "CIBERSORT" algorithm to investigate the differential infiltration of immune cells between the EPR and HC groups. This analysis was visually represented using Heat maps (Fig. 6A) and Box-whisker Plots (Fig. 6B). Our findings revealed that the EPR group exhibited increased infiltration of Macrophages M0, Macrophages M2, Activated Mast cells, Neutrophils, Monocytes, Activated Dendritic cells and Activated T cells CD4 memory cells compared to the HC group, while there was a decrease in the infiltration of Eosinophils, Resting Mast cells, T cells CD8, Naive T cells CD4, Naive B cells, and Resting NK cells (Fig. 6B). Additionally, we conducted a correlation analysis between the identified marker genes and infiltrated immune cells, which demonstrated a significant association between TCN2 and LY6E with various immune cell types (Fig. 6C).

Identification of potentially effective drugs

Moreover, the "Enrichr" database was utilized for the analysis of potential drugs targeting TCN2 or LY6E. The screening process involved a comprehensive evaluation of P-value, Adjusted P-value, and Combined Score. Regrettably, no potential drugs targeting LY6E were identified due to an Adjusted P-value > 0.05 (Figure. S4B). However, the analysis did reveal 3′-Azido-3′-deoxythymidine (CAS: 30516-87-1), Methaneseleninic acid (CAS: 28274-57-9), Dexamethasone (CAS: 50-02-2), Theophylline (CAS: 58-55-9), and Methotrexate (CAS: 59-05-2) as potential drugs targeting TCN2 (Figure. S4A). In order to further explored the interaction of TCN2 with potential targeted agents, the 3D structures of 3'-Azido-3′-deoxythymidine (PubChem ID: 35370), Dexamethasone (PubChem ID: 5743), Theophylline (PubChem ID:

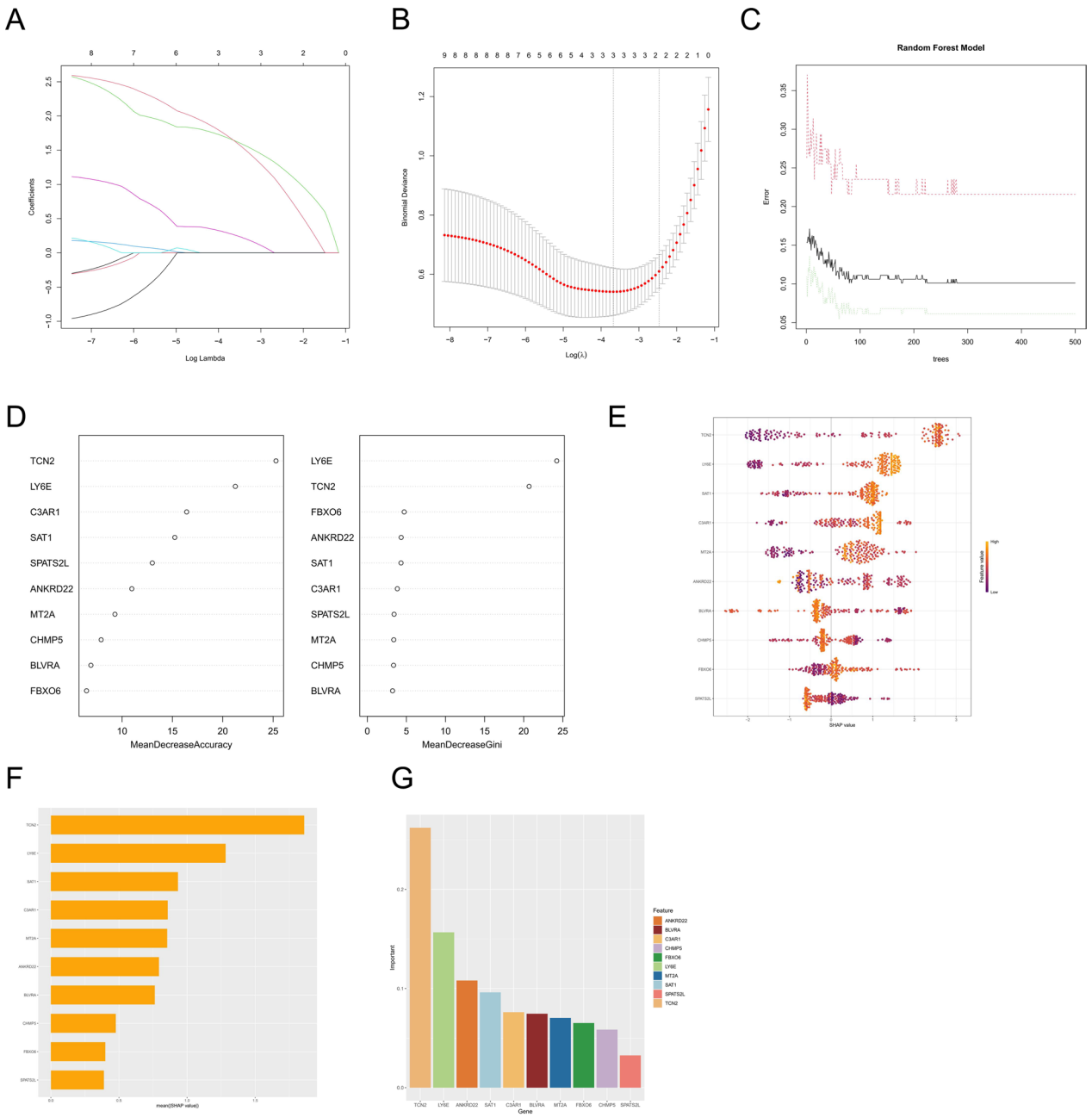

Fig. 4 Detection of novel biomarkers using machine-learning algorithms. **A, B** Based on LASSO regression algorithm to screen biomarkers. **C, D** Based on RF algorithm to screen biomarkers. **E–G** Based on XGBoost algorithm to screen biomarkers

2153) and Methotrexate (PubChem ID: 126941) were obtained from the PubChem database. Additionally, the 3D structure of Methaneseleninic acid (ChemSpider ID: 141936) was acquired from the ChemSpider database. Furthermore, the 3D structure of TCN2 (PDB ID: 2BB5) was retrieved from the PDB database. Subsequently, the "AutoDock Vina" software was used to perform molecular docking analysis between the target protein and potential drugs. The findings revealed that 3'-Azido-3'-deoxythymidine, Dexamethasone, Theophylline and Methotrexate exhibited an affinity with TCN2 < − 5 kcal/mol, indicating a relatively strong binding confidence between TCN2 and these four compounds (Figure S5A–D). Conversely, Methaneseleninic acid displayed an affinity with TCN2 > − 5 kcal/mol, suggesting a lower level of confidence in the binding interaction (Figure S5E). Next,

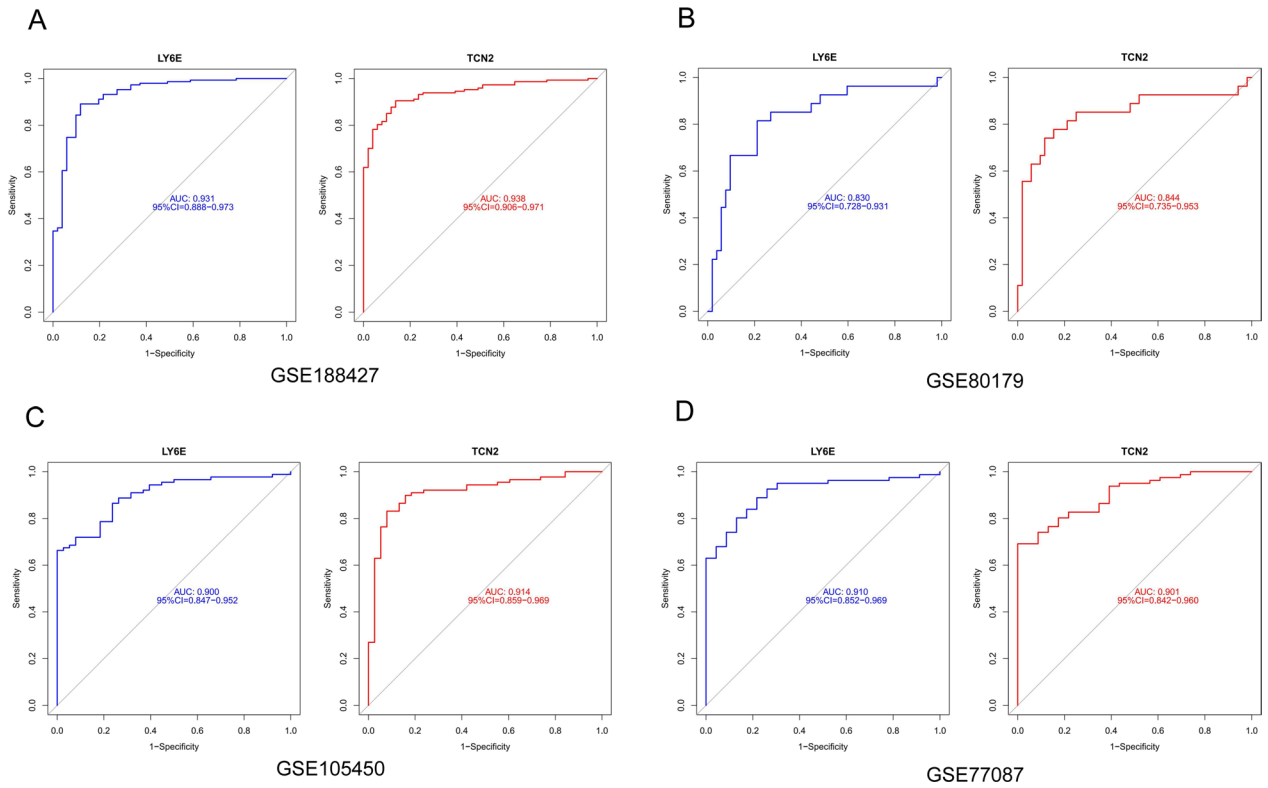

Fig. 5 LY6E and TCN2 diagnostic ROC curves for discriminating RSV infected from healthy controls. **A** ROC analysis for LY6E and TCN2 in dataset GSE188427. **B** ROC analysis for LY6E and TCN2 in dataset GSE80179. **C** ROC analysis for LY6E and TCN2 in dataset GSE105450. **D** ROC analysis for LY6E and TCN2 in dataset GSE77087

the visualization of the binding interactions between TCN2 and the potential drugs was performed using the "PyMOL" software (Fig. 7A–D). Finally, we further revealed the antiviral function of these four drugs, and our data showed 3′-Azido-3′-deoxythymidine (Fig. 7E), Methotrexate (Fig. 7G) and Theophylline (Fig. 7H) inhibited RSV infection in vitro, whereas Dexamethasone (Fig. 7F) promoted RSV infection in vitro.

Expression and role of LY6E and TCN2 in RSV infection

In the aforementioned study, it was discovered that LY6E and TCN2 were upregulated in EPR, and their diagnostic utility for RSV infection was preliminarily confirmed. Notably, LY6E and TCN2 mRNA levels were significantly elevated in the PBMCs of patients infected with RSV compared to healthy control subjects (Fig. 8A, C). Furthermore, ROC analysis revealed that the AUC for LY6E was 0.924 (Fig. 8B), and for TCN2, it was 0.896 (Fig. 8D). These findings suggested that LY6E and TCN2 possessed substantial diagnostic value in the early-stages of RSV infection. Next, an investigation was conducted to examine the impact of RSV on the expression of LY6E and TCN2 through RT-qPCR in vitro. Following RSV infection, there was a gradual increase in LY6E and TCN2 mRNA levels observed in both A549 (Fig. 8E) and BEAS-2B (Fig. 8F) cells. Then, we employed RSV to analyze the antiviral function of LY6E and TCN2. We noticed that overexpression of LY6E demonstrated a significant inhibition of RSV infection in both A549 (Fig. 9A) and BEAS-2B cells (Fig. 9B). Similarly, TCN2 also exhibited inhibitory effects on RSV infection in both A549 (Fig. 9C) and BEAS-2B cells (Fig. 9D). We constructed specific shRNAs to effectively reduce the expression of endogenous LY6E and TCN2. The efficacy of LY6E and TCN2 knockdown was validated using RT-qPCR (Figure S6). Subsequent analysis revealed that the suppression of endogenous LY6E (Fig. 9E) and TCN2 (Fig. 9F) facilitated an increase in RSV infection. To directly observed the impact of LY6E and TCN2 on RSV infection, an immunofluorescence assay was carried out in BEAS-2B (Fig. 9G) and Hep2 (Fig. 9H) cells infected with RSV-mCherry, a strain of RSV L19 containing a mCherry gene. The results indicated that overexpression of LY6E and TCN2 resulted in decreased mCherry signals, demonstrating their ability to inhibit RSV infection. Finally, the antiviral function of LY6E and TCN2 was confirmed through western blot analysis (Fig. 9I).

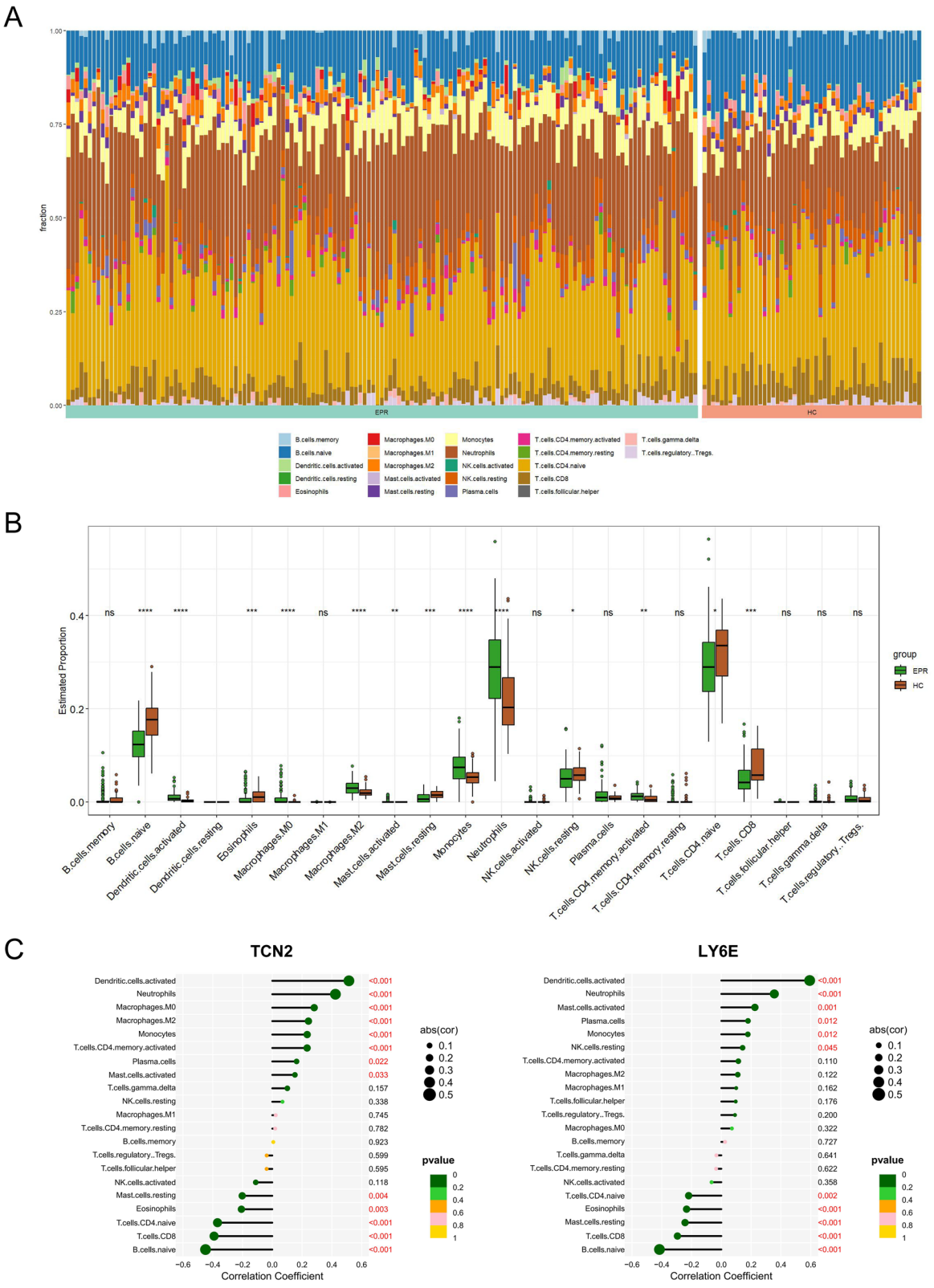

Fig. 6 Immune cell infiltration analysis. **A** The proportion of immune cells in the EPR and HC groups. **B** The CIBERSORT-based boxplot demonstrated a significant difference in immune infiltration patterns between the two groups. **C** Correlation between TCN2 and infiltrating immune cells (left), Correlation between LY6E and infiltrating immune cells (right)

Vitamin B12 (VB12) inhibited RSV infection

We had confirmed that TCN2 had the ability to inhibit RSV infection. Considering that TCN2 is a transport protein for VB12 and it promotes the absorption of VB12 in the body, we sought to investigate the potential role of VB12 in RSV infection. Further analysis demonstrated that the presence of VB12 effectively restricted RSV infection in a dose-dependent manner across various cell lines, such as A549 and Hep2 (Fig. 10A–C). In addition, we found that knocking down endogenous TCN2 expression largely blocked the antiviral function of VB12 (Fig. 10D).

Discussion

RSV is a major factor contributing to hospital admissions for lower respiratory tract infections among children, particularly those under 5 years of age [26, 27]. Presently, the management of pediatric RSV infection predominantly hinges on early detection, prevention, and treatment, underscoring the critical need to enhance the precision of clinical testing for early diagnosis and intervention[28, 29]. The PCR assay and rapid antigen detection are frequently utilized in the diagnosis of pediatric RSV infection. However, PCR assay is associated with drawbacks such as complex procedures, time-consuming and susceptibility to cross-contamination, while rapid antigen detection exhibits limited sensitivity in early-stage pediatric RSV detection. Owing to the aforementioned methodological limitations, these diagnostic methods may fail to identify the optimal treatment window for pediatric RSV infections. Consequently, there is an imperative need to explore novel diagnostic biomarkers for early-stage pediatric RSV detection to enhance diagnostic accuracy. In our study, we identified TCN2 and LY6E as potential biomarkers of EPR due to their high expression in EPR and their potential antiviral biological function.

The EPR dataset was acquired from the GEO database, leading to the identification of 477 DEGs between the EPR and HC groups, with 398 exhibiting upregulation in the EPR group. Enrichment analysis (GO, KEGG) revealed the activation of numerous immune-related signaling pathways in response to RSV infection. Subsequently, we used WGCNA to identify EPR co-expression gene modules and selected the magenta module, which had the maximum positive correlation with EPR and encompassing 338 genes. Additionally, the establishment of a database containing virus-associated genes facilitated the discovery of novel RSV infection-related genes. Fifty genes that exhibited high expression in the EPR group, which had previously been underreported in viral infection studies, were identified as RSV infection-related genes. Subsequently, the GSE80179 dataset was used to further analyze reliable EPR biomarkers, resulting in the identification of 10 EPR Hub Genes. Utilizing three machine-learning algorithms (LASSO, RF, XGBoost), TCN2 and LY6E were identified as potential biomarkers for EPR. Additionally, CIBERSORT analysis revealed significant alterations in immune cell subpopulations in EPR peripheral blood. Moreover, correlation analysis demonstrated that the expression of TCN2 and LY6E correlated with several different immune cell infiltrations.

TCN2, a VB12 binding protein predominantly produced by endothelial cells, has the capacity to bind 10–30% of the Vitamin B12 present in plasma [30]. Upon binding with TCN2, VB12 in plasma forms a complex termed holotranscobalamin. This complex subsequently attaches to the TCN2 receptor (TCII-R) located on the cellular membrane, thereby aiding in the uptake of VB12 into cells [31]. The pivotal role of TCN2 in sustaining red blood cell functionality, DNA synthesis and neurological disorders is noteworthy [32]. Moreover, researchers have demonstrated that TCN2 exhibits high expression levels in a range of solid tumors and is often linked to unfavorable tumor outcomes [30]. Recent investigations have revealed elevated levels of TCN2 in the cerebrospinal fluid of individuals with neuropsychiatric systemic lupus erythematosus (NPSLE), indicating its potential utility as

(See figure on next page.)

Fig. 7 Molecular docking validation of TCN2 with candidate therapeutic agents, followed by an analysis of the antiviral functions of these agents. In this illustration, potentially effective drugs are shown in yellow, and TCN2 is shown in green. Amino acid residues that interact with potentially effective drugs by hydrogen bonding are highlighted in blue. The and yellow dashed line represented a hydrogen bond. **A** 3′-Azido-3′-deoxythymidine, **B** Dexamethasone, **C** Methotrexate, **D** Theophylline. **E** RT–qPCR analysis of RSV F RNA level in BEAS-2B cells pretreated with 3′-Azido-3′-deoxythymidine (0, 1, 5 10, 20 and 50 μM) for 24 h, and then infected with RSV (MOI = 1.0) for 20 h. The relative expression of RSV RNA was normalized to GAPDH mRNA. **F** RT–qPCR analysis of RSV F RNA level in BEAS-2B cells pretreated with Dexamethasone (0, 1, 5 10, 20 and 50 μM) for 24 h, and then infected with RSV (MOI = 1.0) for 20 h. The relative expression of RSV RNA was normalized to GAPDH mRNA. **G** RT–qPCR analysis of RSV F RNA level in BEAS-2B cells pretreated with Methotrexate (0, 0.2, 1 and 5 μM) for 12 h, and then infected with RSV (MOI = 1.0) for 20 h. The relative expression of RSV RNA was normalized to GAPDH mRNA. **H** RT–qPCR analysis of RSV F RNA level in BEAS-2B cells pretreated with Theophylline (0, 1, 5 10, 20 and 50 μM) for 24 h, and then infected with RSV (MOI = 1.0) for 20 h. The relative expression of RSV RNA was normalized to GAPDH mRNA. $^{**}p < 0.01$ and $^{***}p < 0.001$ (one-way analysis of variance). All data are shown as mean ± s.d. of three independent replicates (**A**, **B**)

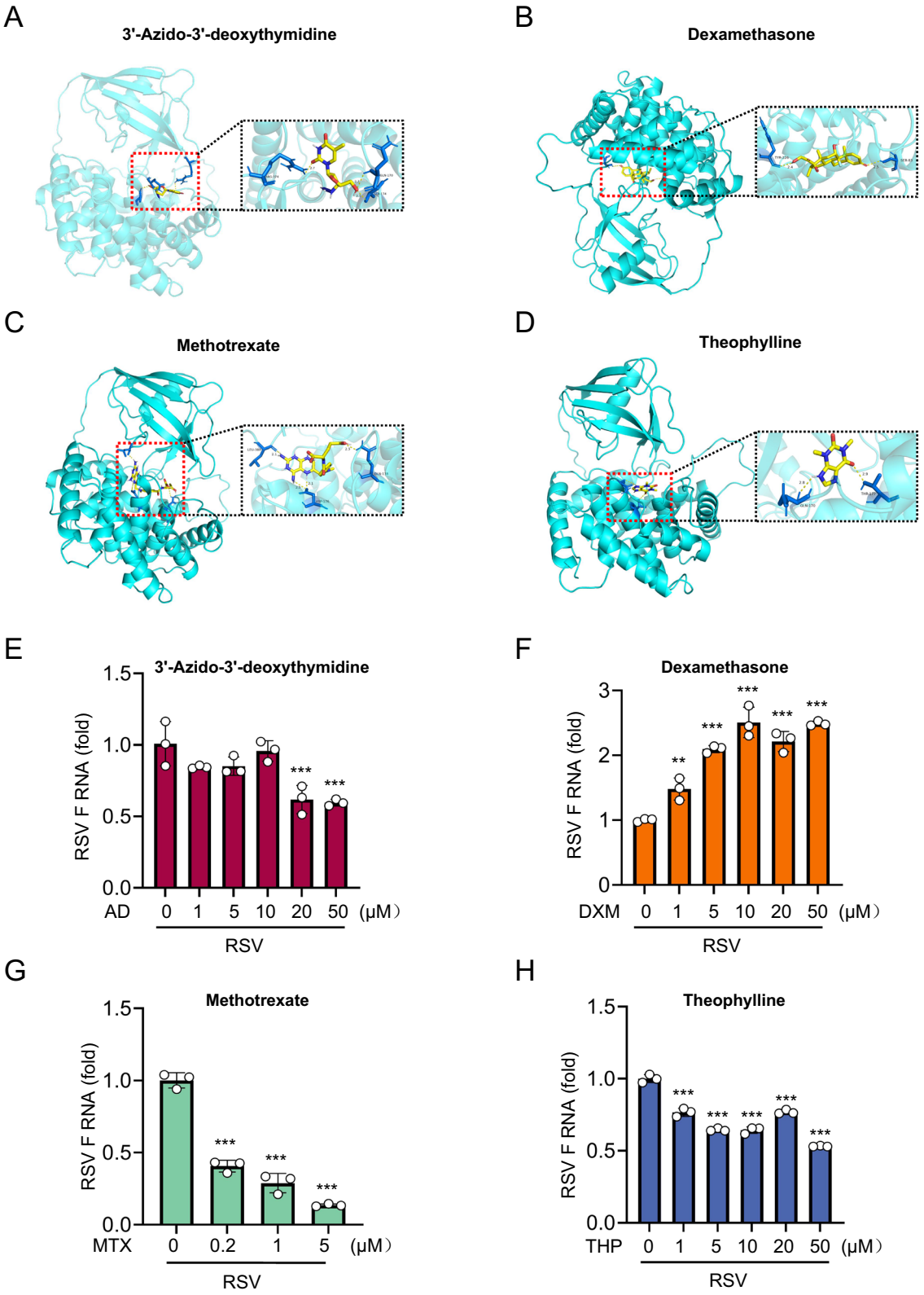

Fig. 7 (See legend on previous page.)

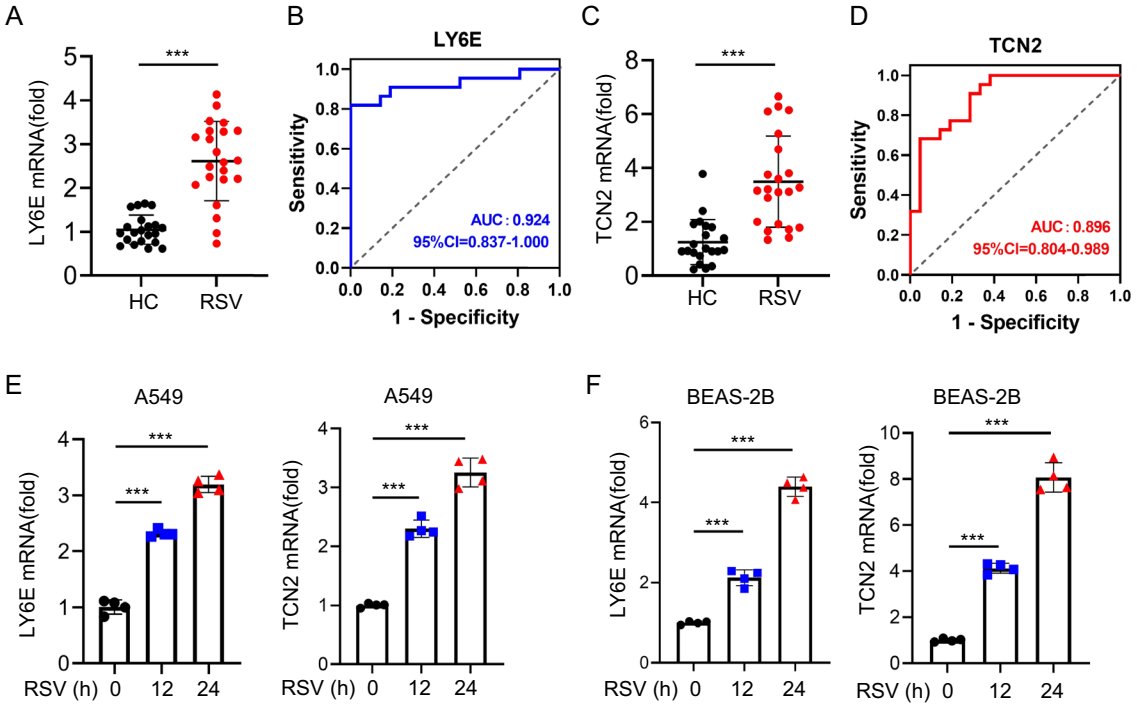

Fig. 8 RSV infection promoted the transcriptional expression of LY6E and TCN2. **A** RT-qPCR analysis of LY6E mRNA levels in human PBMCs from healthy controls (n = 21) and RSV infected patients (n = 23). The relative expression of the LY6E was normalized to GAPDH mRNA. **B** ROC analysis of LY6E expression in healthy controls and RSV infected patients. **C** RT-qPCR analysis of TCN2 mRNA levels in human PBMCs from healthy controls (n = 21) and RSV infected patients (n = 23). The relative expression of the TCN2 was normalized to GAPDH mRNA. **D** ROC analysis of TCN2 expression in healthy controls and RSV infected patients. **E** RT-qPCR analysis of LY6E (Left) and TCN2 (Right) mRNA in A549 cells infected with RSV (MOI = 1.0) for indicated durations. The relative expression of the LY6E and TCN2 genes was normalized to GAPDH mRNA. **F** RT-qPCR analysis of LY6E (Left) and TCN2 (Right) mRNA in BEAS-2B cells infected with RSV (MOI = 1.0) for indicated durations. The relative expression of the LY6E and TCN2 genes was normalized to GAPDH mRNA. ***p < 0.001 (two-tailed unpaired Student's t-test or one-way analysis of variance). All data are shown as mean ± s.d. of four independent replicates (**E**, **F**)

a biomarker for diagnosing NPSLE [33]. Our findings also indicated that EPR enhanced the expression of TCN2 in blood cells. Considering that TCN2 was a secreted protein detectable in serum [34], our study posited TCN2 as a potential serum biomarker for EPR. Furthermore, we conducted experiments to analyze the function of TCN2 in RSV infection, revealing heightened expression in infected cells and demonstrating an antiviral function.

(See figure on next page.)

Fig. 9 LY6E and TCN2 inhibited RSV infection. **A** RT-qPCR analysis of the RSV F (Left) and M2-1 (Right) RNA in A549 cells transfected with pcDNA3.1 vector or Flag-LY6E followed by infection with RSV (MOI = 1.0) for 20 h. The relative expression of RSV RNA was normalized to GAPDH mRNA. **B** RT-qPCR analysis of the RSV F (Left) and M2-1 (Right) RNA in BEAS-2B cells transfected with pcDNA3.1 vector or Flag-LY6E followed by infection with RSV (MOI = 1.0) for 20 h. The relative expression of RSV RNA was normalized to GAPDH mRNA. **C** RT-qPCR analysis of the RSV F (Left) and M2-1 (Right) RNA in A549 cells transfected with pcDNA3.1 vector or Flag-TCN2 followed by infection with RSV (MOI = 1.0) for 20 h. The relative expression of RSV RNA was normalized to GAPDH mRNA. **D** RT-qPCR analysis of the RSV F (Left) and M2-1 (Right) RNA in BEAS-2B cells transfected with pcDNA3.1 vector or Flag-TCN2 followed by infection with RSV (MOI = 1.0) for 20 h. The relative expression of RSV RNA was normalized to GAPDH mRNA. **E** RT-qPCR analysis of the RSV F (Left) and M2-1 (Right) RNA in BEAS-2B cells transfected with pLVX-shRNA2 vector or shLY6E followed by infection with RSV (MOI = 1.0) for 20 h. The relative expression of RSV RNA was normalized to GAPDH mRNA. **F** RT-qPCR analysis of the RSV F (Left) and M2-1 (Right) RNA in BEAS-2B cells transfected with pLVX-shRNA2 vector or shTCN2 followed by infection with RSV (MOI = 1.0) for 20 h. The relative expression of RSV RNA was normalized to GAPDH mRNA. **G** Fluorescence microscopy analysis of RSV-mCherry in BEAS-2B cells transfected with pcDNA3.1 vector or Flag-LY6E followed by infection with RSV-mCherry (MOI = 1.0) for 20 h. Scale bars, 200 μm. **H** Fluorescence microscopy analysis of RSV-mCherry in Hep2 cells transfected with pcDNA3.1 vector or Flag-TCN2 followed by infection with RSV-mCherry (MOI = 1.0) for 20 h. Scale bars, 200 μm. **I** Western blot analysis of the RSV M2-1 protein in A549 cells transfected with pcDNA3.1 vector or Flag-LY6E or Flag-TCN2 followed by infection with RSV (MOI = 1.0) for 20 h. **p < 0.01 and ***p < 0.001 (two-tailed unpaired Student's t-test). All data are shown as mean ± s.d. of four independent replicates (**A**–**F**)

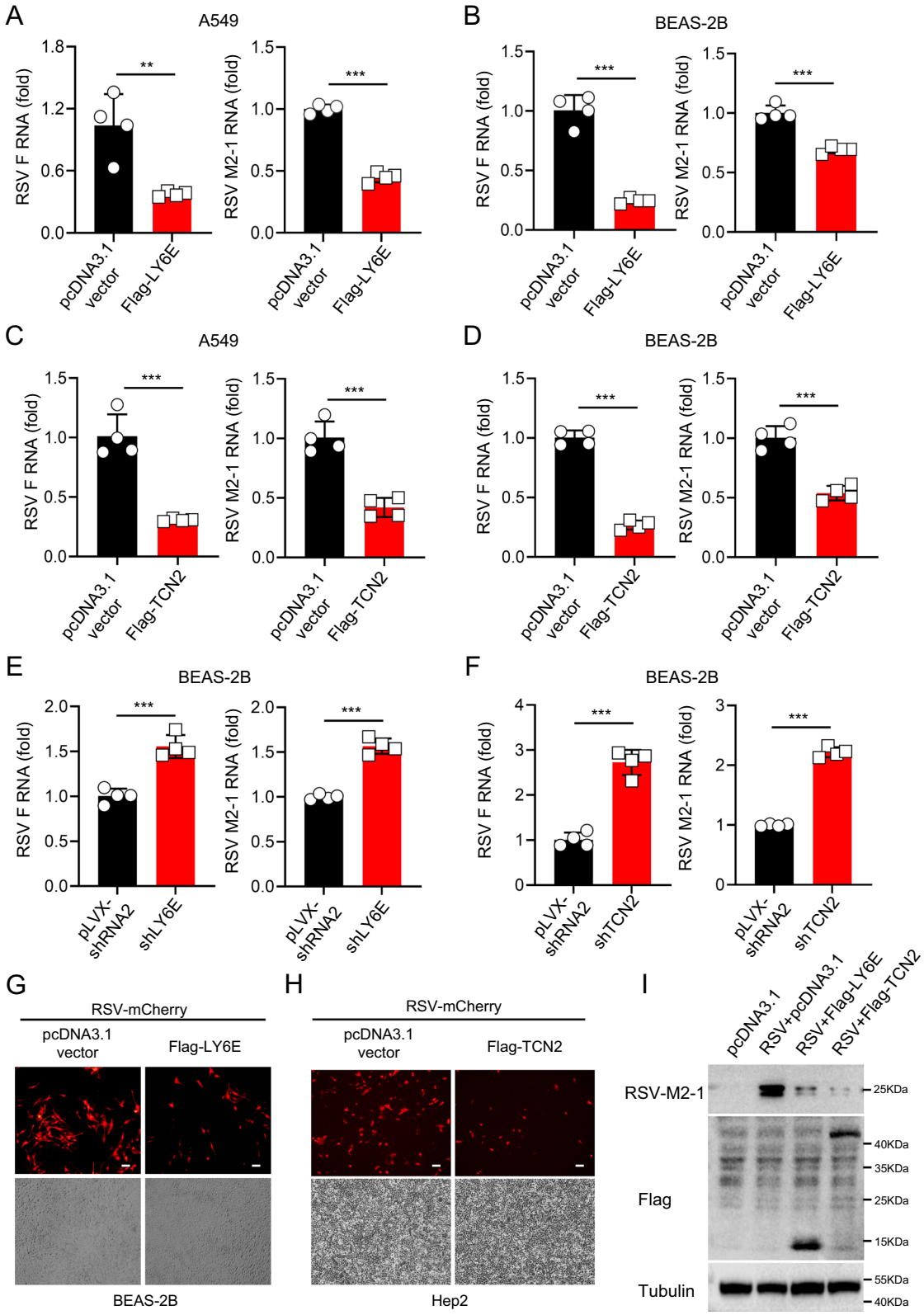

Fig. 9 (See legend on previous page.)

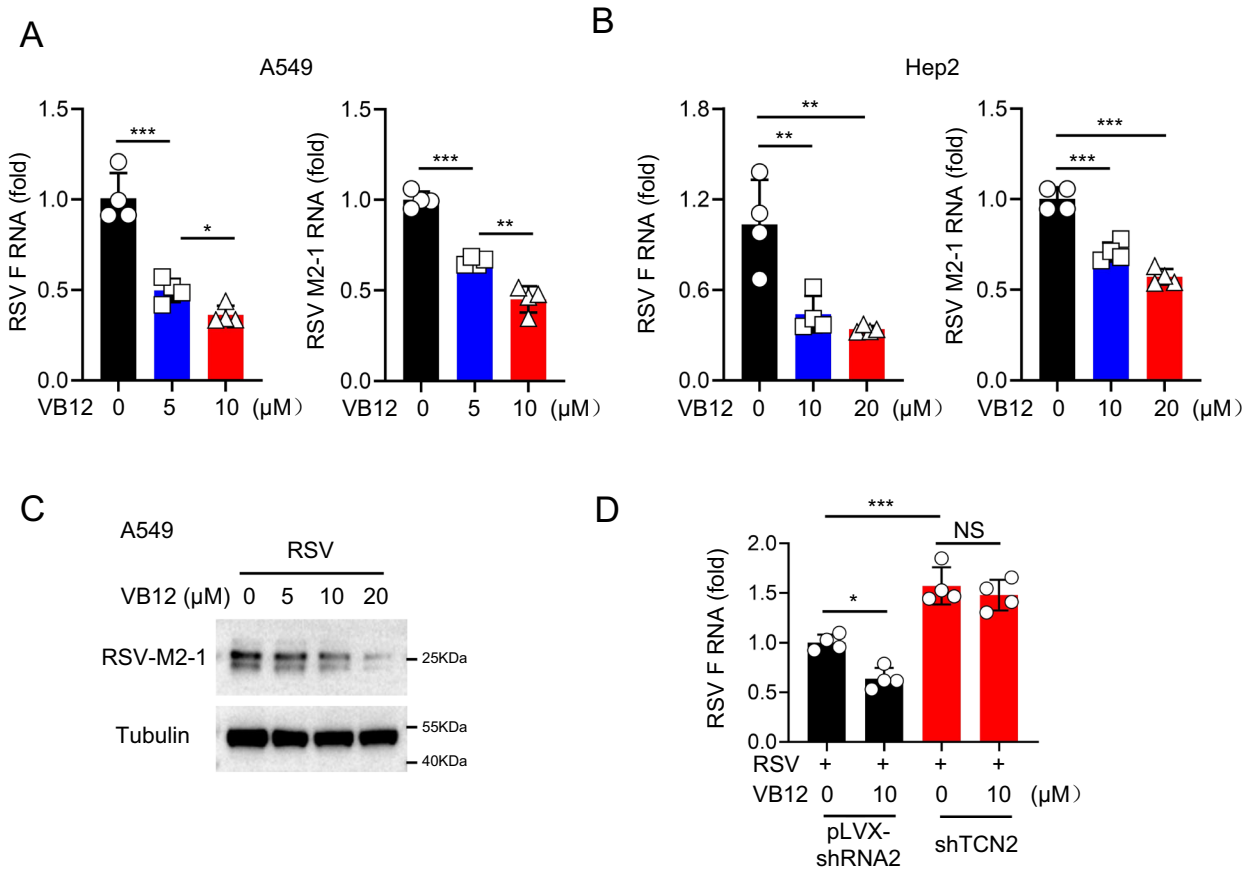

Fig. 10 Vitamin B12 inhibited RSV infection. **A** RT–qPCR analysis of RSV F (Left) and M2-1 (Right) RNA in A549 cells pretreated with VB12 (0, 5 and 10 μM) for 24 h, and then infected with RSV (MOI = 1.0) for 20 h. The relative expression of RSV RNA was normalized to GAPDH mRNA. **B** RT–qPCR analysis of RSV F (Left) and M2-1 (Right) RNA in Hep2 cells pretreated with VB12 (0, 10 and 20 μM) for 24 h, and then infected with RSV (MOI = 1.0) for 20 h. The relative expression of RSV RNA was normalized to GAPDH mRNA. **C** Western blot analysis of RSV M2-1 protein in A549 cells pretreated with VB12 (0, 5, 10 and 20 μM) for 24 h, and then infected with RSV (MOI = 1.0) for 20 h. **D** RT-qPCR analysis of the RSV F RNA in BEAS-2B cells transfected with pLVX-shRNA2 vector or shTCN2 and then treated with VB12 (10 μM) for 24 h, followed by infection with RSV (MOI = 1) for 20 h. *$p < 0.05$, **$p < 0.01$ and ***$p < 0.001$ (two-tailed unpaired Student's t-test or one-way analysis of variance). All data are shown as mean ± s.d. of four independent replicates (**A**, **B**, **D**)

Studies have demonstrated that VB12 plays a significant role in regulating host antiviral immunity. Specifically, VB12 has been shown to increase CD4 T cell counts in individuals with HIV infection and improve the antiviral efficacy of interferon-alpha and ribavirin in patients with chronic hepatitis C virus infection undergoing antiviral therapy [35–37]. Additionally, several researchers suggest that supplementation with VB12 may serve as a promising adjuvant therapy for the treatment of COVID-19 infections [38]. Collectively, these studies elucidate the potential antiviral properties of VB12. Our study revealed that TCN2 possesses the capability to impede RSV infection, as it serves as a carrier protein for VB12, facilitating its absorption within the organism. Subsequently, we conducted an analysis on the impact of VB12 on RSV infection, which demonstrated its inhibitory effect on the RSV infection.

LY6E, a glycosylphosphatidylinositol (GPI)-anchored cell surface protein, has been the subject of numerous studies investigating its role in host antiviral immunity [39]. For example, LY6E can either promote or inhibit HIV infection depending on the levels of CD4 expression on T cells [40]. Additionally, LY6E can promote the infection of viruses such as dengue virus (DENV), Zika virus (ZIKV), influenza A virus (IAV), and vesicular stomatitis virus (VSV), while also showing potential in limiting the infection of multiple coronaviruses [41–45]. These studies indicate that the role of LY6E in viral infection is multifaceted. We discovered that LY6E was prominently expressed in EPR, aligning with the observations made by BrittonA Strickland in the cotton rat model [46]. We evaluated the impact of LY6E on RSV infection to illustrate its antiviral function,

further enriching the function of LY6E in host antiviral immunity.

The "CIBERSORT" package was used to analyze the immune infiltration process in early-stage pediatric RSV infection, aiming to enhance comprehension of the host immune response to RSV. Furthermore, alterations in immune cell infiltration may be associated with the advancement of EPR. Our findings indicated an elevation in the immune infiltration of DC cells, macrophages, mast cells, monocytes and neutrophils during EPR, with a positive correlation observed between the expression of TCN2 and LY6E and the infiltration of these cells. These suggested potential significant roles for TCN2 and LY6E in the activation of host immune cells.

Conclusion

Here, we analyzed multiple pediatric RSV infection datasets, identified LY6E and TCN2 as potential diagnostic biomarkers for EPR patients through integrated bioinformatics methods, which were validated using internal and external datasets to confirm their diagnostic significance. Moreover, our data from PBMCs of RSV patients confirmed the diagnostic value of LY6E and TCN2 for RSV infection. Next, we demonstrated that RSV infection upregulated the transcriptional expression of LY6E and TCN2 in cells, and highlighting their antiviral properties. Importantly, we demonstrated the antiviral function of a promising small molecule compound, VB12. Altogether, our study may provide potential diagnostic candidate genes for EPR patients and may provide additional insights for effective clinical treatment strategies.

Abbreviations

RSV	Respiratory syncytial virus
GEO	Gene expression omnibus
DEGs	Differentially expressed genes
EPR	Early-stage pediatric RSV infection
LY6E	Lymphocyte antigen 6E
TCN2	Transcobalamin-2
AD	3′-Azido-3′-deoxythymidine
DXM	Dexamethasone
MTX	Methotrexate
THP	Theophylline
VB12	Vitamin B12
WGCNA	Weighted Gene Co-expression Network Analysis
GO	Gene ontology
KEGG	Kyoto Encyclopedia of Genes and Genomes
BP	Biological progress
CC	Cellular component
MF	Molecular function
LASSO	Least absolute shrinkage and selection operator
RF	Random forest
XGBoost	EXtreme Gradient Boosting

Supplementary Information

The online version contains supplementary material available at https://doi.org/10.1186/s12967-024-05677-8.

Supplementary Material 1.

Acknowledgements

Thanks to Wuxi No. 2 People's Hospital Clinical Medical Research Center for the good scientific research instruments. Thanks to the lab members for valuable discussions and suggestions.

Author contributions

Xiangjie Chen and Fang Gong conceived and designed the projects. Xiangjie Chen, Xiaoping Li and Xianyan Ji performed most of the experiments and data analysis. Bochun Cao, Lin Wan, Yingying Jiang and Lu Zhou performed most of the bioinformatics analysis. Xiangjie Chen wrote the manuscript and Menglu Li improved the manuscript. All authors read and approved the final manuscript.

Funding

This work was supported by the Foundation for the Natural Science Foundation of China (82270034, 82302654), Natural Science Foundation of Jiangsu Province (SBK2023044153), Top Talent Support Program for young and middle-aged people of Wuxi Health Committee (BJ2023028), Young Scholars of Wuxi Municipal Health Commission (Q202228), the "Taihu Light" technical research basic project (K20231058), Boxi Youth Natural Science Foundation (2023012).

Availability of data and materials

All data are available and the correspondent can be contacted if requested.

Declarations

Ethics approval and consent to participate

The research was conducted in strict adherence to a protocol approved by the Ethics Committee of Jiangnan University Medical Center, with informed consent obtained from all participants.

Consent for publication

All authors approved the final manuscript and the submission to this journal.

Competing interests

The authors declare no competing interests.

Author details

[1]Department of Laboratory Medicine, Wuxi No. 2 People's Hospital, Wuxi, Jiangsu, China. [2]State Key Laboratory of Food Science and Technology, Jiangnan University, Wuxi, Jiangsu, China. [3]Wuxi School of Medicine, Jiangnan University, Wuxi, Jiangsu, China. [4]Department of Laboratory Medicine, The First Affiliated Hospital of Soochow University, Soochow University, Suzhou, China. [5]NHC Key Laboratory of Enteric Pathogenic Microbiology, Jiangsu Provincial Center for Disease Control and Prevention, Nanjing, China. [6]Clinical Medical Research Center, Wuxi No. 2 People's Hospital, Wuxi, Jiangsu, China.

Received: 10 June 2024 Accepted: 6 September 2024
Published online: 23 September 2024

References

1. Guzmán Molina C, Rodríguez-Belvís MV, Coroleu Bonet A, Vall Combelles O, García-Algar O. Antibiotics in respiratory tract infections in hospital pediatric emergency departments. Arch Bronconeumol. 2014;50(9):375–8.
2. Tenenbaum T. Respiratory tract infections in children. Pathogens. 2021;10(12).
3. Qiu X, Xu S, Lu Y, Luo Z, Yan Y, Wang C, Ji J. Development of mRNA vaccines against respiratory syncytial virus (RSV). Cytokine Growth Factor Rev. 2022;68:37–53.
4. Esposito S, Abu Raya B, Baraldi E, Flanagan K, Martinon Torres F, Tsolia M, Zielen S. RSV prevention in all infants: which is the most preferable strategy? Front Immunol. 2022;13: 880368.
5. Ramagopal G, Brow E, Mannu A, Vasudevan J, Umadevi L. Demographic, clinical and hematological profile of children with bronchiolitis: a comparative study between respiratory synctial virus [RSV] and [Non RSV] groups. J Clin Diagn Res. 2016;10(8):Sc05-08.

6. Walker CLF, Rudan I, Liu L, Nair H, Theodoratou E, Bhutta ZA, O'Brien KL, Campbell H, Black RE. Global burden of childhood pneumonia and diarrhoea. Lancet. 2013;381(9875):1405–16.
7. Stinson RJ, Morice AH, Sadofsky LR. Modulation of transient receptor potential (TRP) channels by plant derived substances used in over-the-counter cough and cold remedies. Respir Res. 2023;24(1):45.
8. Guo-Parke H, Canning P, Douglas I, Villenave R, Heaney LG, Coyle PV, Lyons JD, Shields MD, Power UF. Relative respiratory syncytial virus cytopathogenesis in upper and lower respiratory tract epithelium. Am J Respir Crit Care Med. 2013;188(7):842–51.
9. Nam HH, Ison MG. Respiratory syncytial virus infection in adults. BMJ. 2019;366: l5021.
10. Lin CY, Hwang D, Chiu NC, Weng LC, Liu HF, Mu JJ, Liu CP, Chi H. Increased detection of viruses in children with respiratory tract infection using PCR. Int J Environ Res Public Health. 2020;17(2):564.
11. Lee DH, Kim J, Ryu S, Kim J, Han E, Choi HJ. Clinical utility of SARS-CoV-2 rapid antigen test in the Emergency Department. Clin Lab. 2023;69(11).
12. Nassenstein C, Schulte-Herbrüggen O, Renz H, Braun A. Nerve growth factor: the central hub in the development of allergic asthma? Eur J Pharmacol. 2006;533(1–3):195–206.
13. Huang X, Li F, Wang Y, Jia X, Jia N, Xiao F, Sun C, Fu J, Chen M, Cui X, et al. Multi-omics analysis reveals underlying host responses in pediatric respiratory syncytial virus pneumonia. iScience. 2023;26(4):106329.
14. Brown PM, Schneeberger DL, Piedimonte G. Biomarkers of respiratory syncytial virus (RSV) infection: specific neutrophil and cytokine levels provide increased accuracy in predicting disease severity. Paediatr Respir Rev. 2015;16(4):232–40.
15. Wu W, Choi EJ, Lee I, Lee YS, Bao X. Non-coding RNAs and their role in respiratory syncytial virus (RSV) and human metapneumovirus (hMPV) infections. Viruses. 2020;12(3):345.
16. Inchley CS, Sonerud T, Fjærli HO, Nakstad B. Nasal mucosal microRNA expression in children with respiratory syncytial virus infection. BMC Infect Dis. 2015;15:150.
17. Huang J, Chen Z, Ye Y, Shao Y, Zhu P, Li X, Ma Y, Xu F, Zhou J, Wu M, et al. DTX3L enhances type I interferon antiviral response by promoting the ubiquitination and phosphorylation of TBK1. J Virol. 2023;97(6): e0068723.
18. Jans J, Unger WWJ, Vissers M, Ahout IML, Schreurs I, Wickenhagen A, de Groot R, de Jonge MI, Ferwerda G. Siglec-1 inhibits RSV-induced interferon gamma production by adult T cells in contrast to newborn T cells. Eur J Immunol. 2018;48(4):621–31.
19. Reel PS, Reel S, Pearson E, Trucco E, Jefferson E. Using machine learning approaches for multi-omics data analysis: a review. Biotechnol Adv. 2021;49: 107739.
20. Nguyen TB, Do DN, Nguyen-Thi ML, Hoang-The H, Tran TT, Nguyen-Thanh T. Identification of potential crucial genes and key pathways shared in Inflammatory Bowel Disease and cervical cancer by machine learning and integrated bioinformatics. Comput Biol Med. 2022;149: 105996.
21. Yu R, Zhang J, Zhuo Y, Hong X, Ye J, Tang S, Zhang Y. Identification of diagnostic signatures and immune cell infiltration characteristics in rheumatoid arthritis by integrating bioinformatic analysis and machine-learning strategies. Front Immunol. 2021;12: 724934.
22. Chang CH, Lin CH, Lane HY. Machine learning and novel biomarkers for the diagnosis of Alzheimer's disease. Int J Mol Sci. 2021;22(5):2761.
23. Liu J, Jin L, Chen X, Yuan Y, Zuo Y, Miao Y, Feng Q, Zhang H, Huang F, Guo T, et al. USP12 translocation maintains interferon antiviral efficacy by inhibiting CBP acetyltransferase activity. PLoS Pathog. 2020;16(1): e1008215.
24. Chen X, Zhao Q, Xu Y, Wu Q, Zhang R, Du Q, Miao Y, Zuo Y, Zhang HG, Huang F, et al. E3 ubiquitin ligase MID1 ubiquitinates and degrades type-I interferon receptor 2. Immunology. 2022;167(3):398–412.
25. Langfelder P, Horvath S. WGCNA: an R package for weighted correlation network analysis. BMC Bioinformatics. 2008;9:559.
26. Li Y, Wang X, Blau DM, Caballero MT, Feikin DR, Gill CJ, Madhi SA, Omer SB, Simões EAF, Campbell H, et al. Global, regional, and national disease burden estimates of acute lower respiratory infections due to respiratory syncytial virus in children younger than 5 years in 2019: a systematic analysis. Lancet. 2022;399(10340):2047–64.
27. Shi T, McAllister DA, O'Brien KL, Simoes EAF, Madhi SA, Gessner BD, Polack FP, Balsells E, Acacio S, Aguayo C, et al. Global, regional, and national disease burden estimates of acute lower respiratory infections due to respiratory syncytial virus in young children in 2015: a systematic review and modelling study. Lancet. 2017;390(10098):946–58.
28. Zhang XL, Zhang X, Hua W, Xie ZD, Liu HM, Zhang HL, Chen BQ, Chen Y, Sun X, Xu Y, et al. Expert consensus on the diagnosis, treatment, and prevention of respiratory syncytial virus infections in children. World J Pediatr. 2024;20(1):11–25.
29. Griffiths C, Drews SJ, Marchant DJ. Respiratory syncytial virus: infection, detection, and new options for prevention and treatment. Clin Microbiol Rev. 2017;30(1):277–319.
30. Lacombe V, Lenaers G, Urbanski G. Diagnostic and therapeutic perspectives associated to cobalamin-dependent metabolism and transcobalamins' synthesis in solid cancers. Nutrients. 2022;14(10):2058.
31. Mitchell ES, Conus N, Kaput J. B vitamin polymorphisms and behavior: evidence of associations with neurodevelopment, depression, schizophrenia, bipolar disorder and cognitive decline. Neurosci Biobehav Rev. 2014;47:307–20.
32. Kose E, Besci O, Gudeloglu E, Suncak S, Oymak Y, Ozen S, Isguder R. Transcobalamin II deficiency in twins with a novel variant in the TCN2 gene: case report and review of literature. J Pediatr Endocrinol Metab. 2020;33(11):1487–99.
33. Ni J, Chen C, Wang S, Liu X, Tan L, Lu L, Fan Y, Hou Y, Dou H, Liang J. Novel CSF biomarkers for diagnosis and integrated analysis of neuropsychiatric systemic lupus erythematosus: based on antibody profiling. Arthritis Res Ther. 2023;25(1):165.
34. Fràter-Schröder M, Porck HJ, Erten J, Müller MR, Steinmann B, Kierat L, Arwert F. Synthesis and secretion of the human vitamin B12-binding protein, transcobalamin II, by cultured skin fibroblasts and by bone marrow cells. Biochim Biophys Acta. 1985;845(3):421–7.
35. Semeere AS, Nakanjako D, Ddungu H, Kambugu A, Manabe YC, Colebunders R. Sub-optimal vitamin B-12 levels among ART-naïve HIV-positive individuals in an urban cohort in Uganda. PLoS ONE. 2012;7(7): e40072.
36. Balfour L, Spaans JN, Fergusson D, Huff H, Mills EJ, la Porte CJ, Walmsley S, Singhal N, Rosenes R, Tremblay N, et al. Micronutrient deficiency and treatment adherence in a randomized controlled trial of micronutrient supplementation in ART-naïve persons with HIV. PLoS ONE. 2014;9(1): e85607.
37. Rocco A, Compare D, Coccoli P, Esposito C, Di Spirito A, Barbato A, Strazzullo P, Nardone G. Vitamin B12 supplementation improves rates of sustained viral response in patients chronically infected with hepatitis C virus. Gut. 2013;62(5):766–73.
38. Batista KS, Cintra VM, Lucena PAF, Manhães-de-Castro R, Toscano AE, Costa LP, Queiroz M, de Andrade SM, Guzman-Quevedo O, Aquino JS. The role of vitamin B12 in viral infections: a comprehensive review of its relationship with the muscle–gut–brain axis and implications for SARS-CoV-2 infection. Nutr Rev. 2022;80(3):561–78.
39. Bacquin A, Bireau C, Tanguy M, Romanet C, Vernochet C, Dupressoir A, Heidmann T. A cell fusion-based screening method identifies glycosylphosphatidylinositol-anchored protein Ly6e as the receptor for mouse endogenous retroviral envelope syncytin-A. J Virol. 2017;91(18).
40. Yu J, Liang C, Liu SL. CD4-dependent modulation of HIV-1 entry by LY6E. J Virol. 2019;93(7).
41. Yu J, Liu SL. Emerging role of LY6E in virus–host interactions. Viruses. 2019;11(11):1020.
42. Mar KB, Rinkenberger NR, Boys IN, Eitson JL, McDougal MB, Richardson RB, Schoggins JW. LY6E mediates an evolutionarily conserved enhancement of virus infection by targeting a late entry step. Nat Commun. 2018;9(1):3603.
43. Pfaender S, Mar KB, Michailidis E, Kratzel A, Boys IN, V'Kovski P, Fan W, Kelly JN, Hirt D, Ebert N, et al. LY6E impairs coronavirus fusion and confers immune control of viral disease. Nat Microbiol. 2020;5(11):1330–9.
44. Mar KB, Wells AI, Caballero Van Dyke MC, Lopez AH, Eitson JL, Fan W, Hanners NW, Evers BM, Shelton JM, Schoggins JW. LY6E is a pan-coronavirus restriction factor in the respiratory tract. Nat Microbiol. 2023;8(8):1587–99.
45. Zhao X, Zheng S, Chen D, Zheng M, Li X, Li G, Lin H, Chang J, Zeng H, Guo JT. LY6E restricts entry of human coronaviruses, including currently pandemic SARS-CoV-2. J Virol. 2020;94(18).
46. Strickland BA, Rajagopala SV, Kamali A, Shilts MH, Pakala SB, Boukhvalova MS, Yooseph S, Blanco JCG, Das SR. Species-specific transcriptomic changes upon respiratory syncytial virus infection in cotton rats. Sci Rep. 2022;12(1):16579.

Publisher's Note